SCIENCE CHINA
Physics, Mechanics & Astronomy

• Article •

January 2012 Vol. 55 No. 1: 125–131
doi: 10.1007/s11433-011-4571-y

Blood flow of an Oldroyd-B fluid in a blood vessel incorporating a Brownian stress

ZAMAN Gul[1*], ISLAM S.[2*], KANG Yong Han[3] & JUNG Il Hyo[3]

[1] *Department of Mathematics, University of Malakand, Chakdara Dir(Lower), Khyber Puhtoonkhwa, Pakistan;*
[2] *Department of Mathematics, COMSATS IIT H-8/1, Islamabad, Pakistan;*
[3] *Department of Mathematics, Pusan National University, Busan 609-735, South Korea*

Received August 27, 2010; accpeted January 31, 2011

The mechanical behavior of non-Newtonian fluids can be modeled by several constitutive differential equations. The Oldroyd model is viewed as one of the successful models for describing the response of a subclass of polymeric liquids, in particular the non-Newtonian behavior exhibited by these fluids. In this paper, we are concerned with the study of the unsteady flows of an incompressible viscoelastic fluid of an Oldroyd-B type in a blood vessel acting on a Brownian force. First we derive the orientation stress tensor considering Hookean dumbbells on Brownian configuration fields. Then we reformulate the three-dimensional Oldroyd-B model with the total stress tensor which consists of the isotropic pressure stress tensor, the shear stress tensor, and the orientation stress tensor. Finally we present the numerical simulations of the model and analyze the effect of the orientation stress tensor in the vessel.

fluid flow, total and orientation stress tensor, Hemodynamics, mathematical models

PACS number(s): 05.40.-a, 03.75Kk

Citation: Zaman G, Islam S, Kang Y H, et al. Blood flow of an Oldroyd-B fluid in a blood vessel incorporating a Brownian stress. Sci China-Phys Mech Astron, 2012, 55: 125–131, doi: 10.1007/s11433-011-4571-y

The cardiovascular system, consisting of the heart and the vascular network of arteries, arterioles, capillaries, venules, and veins, is responsible for the circulation of blood. The vascular network branches into smaller vessels bringing oxygenated blood flow away from the heart. The thickness of the vessel walls decreases as well [1]. The size of the large vessel is between 0.1 mm and 30 mm in diameter and consists of three layers: the intima, media, and the adventitia. There are a number of fundamental categories dividing blood flow. These categories better suggest schemes for the prediction of flow inside the vessel.

Blood exhibits non-Newtonian characteristics mainly due to shear thinning viscosity and viscoelasticity related to stress relaxation and normal stress effects. In particular, in the case of small arteries, arterioles, the microstructure and rheological behavior of blood should not be neglected since the dimension of the blood particles is of the same order as that of the vessels. So blood can be modeled as a homogeneous shear-thinning and viscoelastic fluid characterized by the Oldroyd-B type model.

Therefore, the Oldroyd-B fluid presents one of the simplest constitutive models capable of describing the viscoelastic behavior of dilute polymeric solutions under general flow conditions. The expressions for both steady and unsteady velocity fields for the generalized Oldroyd-B fluid are considered in the vessels [2,3]. It is a well-known observation from designers of wind tunnels, diffusers, and airplanes that if the angle between the wall and the main flow direction is too long, the streamlines of the flow may detach from the wall and create a so-called separated region. In the separated region, the flow is unsteady and the shear stress is lower than that in the unseparated regions [4].

The compressible flow, where the density changes are induced by the pressure changes through the flow field, has a significant effect on the flow. Compressibility effects are usu-

*Corresponding author (ZAMAN Gul: email: talash74@yahoo.com; ISLAM S: email: prond-pak@hotmail.com)

ally associated with high speed flow of gases. We analyze incompressible blood flow by applying the principles of conservation of mass, momentum, and energy together with the equation of state to deduce the variations of velocity, pressure, density, and temperature throughout the blood vessel. In the cardiovascular system, blood flow is under constant interaction with the vessel walls. Many studies have simulated blood flow through rigid arteries. A review on the theoretical developments and new trends in arterial mechanics is given in ref. [5]. Asymmetric flows of non-Newtonian fluids in the symmetric stenosed artery in three dimensions can be found in ref. [6]. Experimental studies on the axisymmetric sphere-wall interaction in both Newtonian and non-Newtonian fluids have been reported in ref. [7]. Mekheimer [8] studied the effect of the induced magnetic field on peristaltic flow of a couple stress fluid. The blood flows through a circular pipe with an impulsive pressure gradient and only a non-zero component of velocity w with the z-axis was introduced in ref. [9] while the blood flow through an axisymmetric stenosis with velocity components u and w in 2-dimensions was presented in ref. [10]. Some of the above researchers and several more have proposed various representative models for blood in small vessels and narrow capillaries by considering a total stress tensor consisting of the isotropic pressure stress tensor and the shear stress tensor in the absence of the orientation stress tensor.

In this paper, we consider a total stress tensor consisting of the isotropic pressure stress tensor, the shear stress tensor, and the orientation stress tensor to understand the dynamics of blood flow inside the vessel. First, we derive the orientation stress tensor from the Brownian force and an equivalent microscopic description of the polymer dynamics in terms of an ensemble of Hookean dumbbells. Then, we reformulate the three-dimensional Oldroyd-B model coupled with the momentum equation and the total stress tensor. Finally, we discuss our numerical analysis of the Oldroyd-B model with velocity components in three dimensions and the momentum equation. Numerical results and discussion show that the effect of the orientation stress tensor in a blood vessel is considerable, although the Brownian force is sufficiently small. We also describe that if there is no stress on the vessel wall then the flow is incompressible representing that the diameter of the vessel is constant.

1 Orientation stress tensor

Blood, often called the river of life, consists of red and white blood cells in an aqueous plasma solution. Plasma, water with various proteins, is dissolved along with ions [11]. The blood generally demonstrates both a viscous and an elastic effect, both of which determine the stress-strain relationship. Such liquids are called viscoelastic. Blood plasma shows viscosity, while whole blood is both viscous and elastic. The viscosity is related to the energy dissipated during blood flow, while elasticity is related to the energy stored during flow due to the orientation and deformation of red blood cells. Blood is a non-Newtonian fluid, meaning that its viscosity is not constant, but depends on the rate of shear stress. At low shear rates, the viscosity increases, and at high shear rates, the viscosity decreases [12].

We consider the flow of blood through a cylindrical blood vessel (vein or artery) with a diameter d and length L. The velocity $\boldsymbol{v}$ of the blood increases along the central axis of the vessel. For a given flow rate Q in a cylindrical vessel of diameter d, the viscosity is known as the apparent viscosity $\eta_{\rm app}$:

$$\eta_{\rm app} = \frac{\pi d^4}{2^3 L}\frac{\Delta p}{Q}, \tag{1}$$

where Δp is the pressure difference between the ends of the vessel. The percentage of the blood volume occupied by red blood cells is called the hematocrit. The relative viscosity $\eta(h, d)$ of blood is a function of the vessel diameter d and hematocrit h [13]. The measurement of blood viscosity in micro vessels is very difficult, while the viscosity of the plasma is approximately 1.2 cP [14] which has Newtonian characteristics. It is evident that red blood cells are responsible for non-Newtonian behavior. The viscosity, or internal friction, of the blood increases as the percentage of cells in the blood increases: more cells mean more friction with greater viscosity. With a normal hematocrit of about 40 (that is, approximately 40% of the blood volume is red blood cells and the remainder plasma), the viscosity of whole blood (cells plus plasma) is about 3 times that of water. On the other hand, the viscosity of plasma alone is about 1.5 times that of water. Although the concentrations and types of proteins in the plasma can affect its viscosity, this has little if any effect on the overall viscosity of whole blood. When the hematocrit rises to 60 or 70, which it often does in patients with polycythemia, or abnormally high red blood cell counts, the blood viscosity can become as high as 10 times that of water. Alternatively, when the hematocrit falls drastically, as it does in patients with anemia (a decreased number of red cells in the blood), blood viscosity can approach that of plasma alone.

In order to derive the orientation stress tensor in blood flow, we consideran equivalent microscopic description of the polymer dynamics in terms of an ensemble of Hookean dumbbells. For the experimental dumbbell model in Brownian configuration fields, we refer the reader to [15]. We consider two spherical beads and connect them together with a linear spring [16]. We set one bead at position $\boldsymbol{x}$ with radius a and another bead at position $\boldsymbol{x}+\boldsymbol{r}$. The spring force $\boldsymbol{F}_{\rm s}$ pulling a bead towards the other beads is $\beta\boldsymbol{r}$. Here $\beta = 3k\Gamma/a^2$ is a spring constant with temperature $\Gamma = 37$°C and the Boltzmann constant k (= 1.38×10^{-23} m^2 kg s^{-2} K^{-1}). The drag force $\boldsymbol{F}_{\rm d}$ from the bead moving through the viscous solvent is given by $\boldsymbol{F}_{\rm d} = -6\pi\eta a({\rm d}\boldsymbol{x}/{\rm d}t - \boldsymbol{v}(\boldsymbol{x}))$. Here, $\boldsymbol{v}(\boldsymbol{x})$ and ${\rm d}\boldsymbol{x}/{\rm d}t$ is the velocity of the fluid and bead, respectively. $\eta = \eta(h, d)$ is the viscosity of the fluid (blood). It is common to neglect inertia because of the small mass of these particles. By using Newton's Second Law, we show that the total force is always approximately zero [17]. Thus, we get

$$\boldsymbol{F}_{\rm tot} = \boldsymbol{F}_{\rm s} + \boldsymbol{F}_{\rm d} + \boldsymbol{F}_{\rm B} \simeq 0, \tag{2}$$

where $\boldsymbol{F}_{\rm tot}$ and $\boldsymbol{F}_{\rm B}$ are the total and the Brownian force, respectively. To find the velocity of the bead at position $\boldsymbol{x}$, let us substitute $\boldsymbol{F}_{\rm s}$ and $\boldsymbol{F}_{\rm d}$ in eq. (2). Then, we get

$$\frac{{\rm d}\boldsymbol{x}}{{\rm d}t} = \frac{k\Gamma}{2\pi\eta a^3}\boldsymbol{r} + \boldsymbol{v}(\boldsymbol{x}) + \frac{1}{6\pi\eta a}\boldsymbol{F}_B(\boldsymbol{x}). \tag{3}$$

Similarly, the velocity ${\rm d}(\boldsymbol{x}+\boldsymbol{r})/{\rm d}t$ at $\boldsymbol{x}+\boldsymbol{r}$ with the spring force, says $-\beta\boldsymbol{r}$ is given:

$$\frac{{\rm d}(\boldsymbol{x}+\boldsymbol{r})}{{\rm d}t} = -\frac{k\Gamma}{2\pi\eta a^3}\boldsymbol{r} + \boldsymbol{v}(\boldsymbol{x}+\boldsymbol{r}) + \frac{1}{6\pi\eta a}\boldsymbol{F}_{\rm B}(\boldsymbol{x}+\boldsymbol{r}). \tag{4}$$

Thus, the velocity difference between the two beads can be written as:

$$\frac{{\rm d}(\boldsymbol{x}+\boldsymbol{r})}{{\rm d}t} - \frac{{\rm d}\boldsymbol{x}}{{\rm d}t} = \frac{{\rm d}\boldsymbol{r}}{{\rm d}t}. \tag{5}$$

If we invoke the locally linear flow assumption, the difference in fluid velocities is approximated by a Taylor series expansion of the first order velocity gradient tensor:

$$\boldsymbol{v}(\boldsymbol{x}+\boldsymbol{r}) - \boldsymbol{v}(\boldsymbol{x}) \simeq \boldsymbol{r}\cdot\nabla\boldsymbol{v}(\boldsymbol{x}).$$

Combining these relationships leads to the following stochastic differential equation for the separation vector:

$$\frac{{\rm d}\boldsymbol{r}}{{\rm d}t} = -\frac{1}{2\tau}\boldsymbol{r} + \boldsymbol{r}\cdot\nabla\boldsymbol{v}(\boldsymbol{x}) + \frac{1}{6\pi\eta a}(\boldsymbol{F}_{\rm B}(\boldsymbol{x}+\boldsymbol{r}) - \boldsymbol{F}_{\rm B}(\boldsymbol{x})), \tag{6}$$

where $2k\Gamma/\pi\eta a^3 = \tau^{-1}$ which represents the inverse relaxation time of the dumbbell. The change in the Brownian force due to collisions of the solvent molecules with the beads is determined by $(\boldsymbol{F}_{\rm B}(\boldsymbol{x}+\boldsymbol{r}) - \boldsymbol{F}_{\rm B}(\boldsymbol{x})){\rm d}t = ({\rm d}B_t, {\rm d}B_t, {\rm d}B_t)$, where ${\rm d}B_t = \tau^{-1/2}(\alpha(t){\rm d}t)^{1/2}$ for some function $\alpha(t) \geqslant 0$. Since the force that crosses the surface of the dumbbell is $\beta\boldsymbol{r}$, if there are m dumbbells per unit volume, then the number crossing the dumbbell surface δS with the normal unit n becomes $m\boldsymbol{r}\cdot n\delta S$. Thus, the extra stress by the dumbbell becomes

$$\sigma^p\cdot n\delta S = \beta\boldsymbol{r}(m\boldsymbol{r}\cdot n\delta S) \Rightarrow \sigma^p = gM.$$

Here, g is a constant, says elastic modulus, σ^p is the polymer extra stress and M is an orientation stress tensor [18]. Now, we take the orientation stress tensor:

$$M(\boldsymbol{x}, t) = E[\boldsymbol{r}(\boldsymbol{x}, t)\,\boldsymbol{r}(\boldsymbol{x}, t)], \tag{7}$$

where, for $\boldsymbol{r} = (r_1, r_2, r_3)$ the tensor, $\boldsymbol{E}$, can be defined by

$$\boldsymbol{E}[\boldsymbol{rr}] = \begin{bmatrix} r_1r_1 & r_1r_2 & r_1r_3 \\ r_2r_1 & r_2r_2 & r_2r_3 \\ r_3r_1 & r_3r_2 & r_3r_3 \end{bmatrix}.$$

We consider the time-step ${\rm d}t$. Then the position $\boldsymbol{x}$ moves to

$$\boldsymbol{x} + {\rm d}\boldsymbol{x} = \boldsymbol{x} + \boldsymbol{v}(\boldsymbol{x}){\rm d}t, \tag{8}$$

where $\boldsymbol{v}(\boldsymbol{x})$ is the fluid velocity. So after the time-step ${\rm d}t$ the orientation stress tensor becomes

$$\begin{aligned} M(\boldsymbol{x}+\boldsymbol{v}(\boldsymbol{x}){\rm d}t, t+{\rm d}t) &= E[(\boldsymbol{r}+{\rm d}\boldsymbol{r})(\boldsymbol{r}+{\rm d}\boldsymbol{r})] \\ &= E[\boldsymbol{rr} + \boldsymbol{r}{\rm d}\boldsymbol{r} + {\rm d}\boldsymbol{rr} + {\rm d}\boldsymbol{r}{\rm d}\boldsymbol{r}] \\ &= E[\boldsymbol{rr}] + E[\boldsymbol{r}{\rm d}\boldsymbol{r}] + E[{\rm d}\boldsymbol{rr}] + E[{\rm d}\boldsymbol{r}{\rm d}\boldsymbol{r}]. \end{aligned} \tag{9}$$

We simplify and keep only terms up to order ${\rm d}t$:

$$\begin{aligned} \boldsymbol{E}[\boldsymbol{r}\,\boldsymbol{r}] &= M(\boldsymbol{x}, t), \\ \boldsymbol{E}[\boldsymbol{r}\,{\rm d}\boldsymbol{r}] &= -\frac{1}{2\tau}M{\rm d}t + M\cdot\nabla\boldsymbol{v}(\boldsymbol{x}){\rm d}t, \\ \boldsymbol{E}[{\rm d}\boldsymbol{r}\,\boldsymbol{r}] &= -\frac{1}{2\tau}M{\rm d}t + (\nabla\cdot\boldsymbol{v}(\boldsymbol{x}))^{\rm T}M{\rm d}t, \\ \boldsymbol{E}[{\rm d}\boldsymbol{r}\,{\rm d}\boldsymbol{r}] &= \tau^{-1}\frac{\alpha(t)}{(6\pi\eta a)^2}I{\rm d}t, \end{aligned} \tag{10}$$

$$M(\boldsymbol{x}+\boldsymbol{v}(\boldsymbol{x}){\rm d}t, t+{\rm d}t) = (\boldsymbol{v}\cdot\nabla)M{\rm d}t + \frac{\partial M}{\partial t}{\rm d}t + M(\boldsymbol{x}, t). \tag{11}$$

Combining eqs. (9)–(11), we get

$$\frac{\partial M}{\partial t} + (\boldsymbol{v}\cdot\nabla)M - M\nabla\boldsymbol{v} - (\nabla\boldsymbol{v})^{\rm T}M = -\frac{1}{\tau}\left(M - \frac{\alpha(t)}{(6\pi\eta a)^2}I\right). \tag{12}$$

We use this equation coupled with the Oldroyd-B fluid and the momentum equation in next section to approach blood flow dynamics in a vessel.

2 The Oldroyd-B fluid in a vessel incorporating a Brownian stress

Many theoretical and experimental formulations have been developed to describe the finite deformation and the nonlinear viscoelasticity of arteries in time dependent flows. Several researchers, for instance [9,10,19,20] have proposed various representative models for blood in small vessels and narrow capillaries by considering a total stress tensor consisting of the isotropic pressure stress tensor and the shear stress tensor with the absence of the orientation stress tensor. The model is extended here to consider the total stress tensor consisting of the isotropic pressure stress tensor, the shear stress tensor, and the orientation stress tensor with a constant g (the elastic modulus). The governing equations of the vessel are, of course, derived by applying conservation of mass, momentum, and energy to the flow through a control volume. The fluid obeys the following equations. Let us consider the total stress tensor σ and the velocity $\boldsymbol{v}$ of the flow with components $\boldsymbol{v}_i$, where $i = 1, 2, 3$ are rectangular co-ordinates. The continuity and the momentum equations for the time-dependent incompressible flow may be written:

$$\begin{aligned} &\nabla\cdot\boldsymbol{v} = 0, \\ &\rho\left(\frac{\partial\boldsymbol{v}}{\partial t} + \boldsymbol{v}\cdot\nabla\boldsymbol{v}\right) = {\rm div}\sigma, \\ &\sigma = -pI + \eta(\nabla\boldsymbol{v} + (\nabla\boldsymbol{v})^{\rm T}) + gM, \end{aligned} \tag{13}$$

where ρ is the density, σ the total stress tensor, η the viscosity of the blood, $\boldsymbol{I}$ is the identity matrix, $-pI$ the isotropic pressure stress tensor, g the elastic modulus (constant), and $\boldsymbol{M}$ the orientation stress tensor.

Now, we derive the Oldroyd-B equations by combining the equation of continuity, the momentum equation, and eq. (12):

$$\begin{aligned} &\nabla\cdot\boldsymbol{v}=0,\\ &\rho\left(\frac{\partial\boldsymbol{v}}{\partial t}+\boldsymbol{v}\cdot\nabla\boldsymbol{v}\right)=\ \mathrm{div}\sigma,\\ &\sigma=-p\boldsymbol{I}+\eta(\nabla\boldsymbol{v}+(\nabla\boldsymbol{v})^{\mathrm{T}})+g\boldsymbol{M},\\ &\frac{\partial\boldsymbol{M}}{\partial t}+(\boldsymbol{v}\cdot\nabla)\boldsymbol{M}-\boldsymbol{M}\nabla\boldsymbol{v}-(\nabla\boldsymbol{v})^{\mathrm{T}}\boldsymbol{M}\\ &\qquad=-\frac{1}{\tau}\left(\boldsymbol{M}-\frac{\alpha(t)}{(6\pi\eta a)^2}\boldsymbol{I}\right). \end{aligned} \tag{14}$$

In fluid dynamics, the time rate of change for a fluid element is usually denoted by D/Dt, and defined by

$$\frac{\mathrm{D}f}{\mathrm{D}t}=\frac{\partial f}{\partial t}+(\boldsymbol{v}\cdot\nabla)f, \tag{15}$$

where D/Dt is often called the material (Lagrangian) derivative. For reformulation of the system (14) in the form of a material derivative D/Dt, we set $\boldsymbol{A}=\nabla\boldsymbol{v},\ \ \mathrm{W}=\boldsymbol{A}+\boldsymbol{A}^{\mathrm{T}},\ \ \mathrm{B}=\eta\mathrm{W}+g\boldsymbol{M}$. In the system (14), the Oldroyd-B equations are then reformulated with the use of non constant viscosity in the form of

$$\begin{aligned} &\nabla\cdot\boldsymbol{v}=0,\\ &\frac{\mathrm{D}M}{\mathrm{D}t}-\boldsymbol{M}\boldsymbol{A}-\boldsymbol{A}^{\mathrm{T}}\boldsymbol{M}=-\frac{1}{\tau}\left(M-\frac{\alpha(t)}{(6\pi\eta a)^2}\boldsymbol{I}\right),\\ &\boldsymbol{B}+\gamma_1\left[\frac{\mathrm{D}\boldsymbol{B}}{\mathrm{D}t}-\boldsymbol{A}\boldsymbol{B}-\boldsymbol{B}\boldsymbol{A}^{\mathrm{T}}\right]\\ &\quad=\eta\left[\mathrm{W}+\gamma_2\left(\frac{\mathrm{DW}}{\mathrm{D}t}-\boldsymbol{A}\mathrm{W}-\mathrm{W}\boldsymbol{A}^{\mathrm{T}}\right)\right]\\ &\qquad+g\boldsymbol{M}-\frac{\gamma_2 g}{\tau}\left(\boldsymbol{M}-\frac{\alpha(t)}{(6\pi\eta a)^2}\boldsymbol{I}\right), \end{aligned} \tag{16}$$

where η is the viscosity and γ_1 and γ_2 are material constants.

Remark There may be general instructions on the possible values for the constants in the system for physical reality. The full Oldroyd-B fluid in the eq. (16) is reduced to the following form (model) in the absence of the orientation stress tensor:

(1) If $\gamma_1=\gamma_2=0$, then the model is reduced to a pure inelastic fluid and the Naveir-Stokes linear model when, in addition η = constant.

(2) For $\gamma_1=\gamma_2\neq 0$, the model is reduced to a Newtonian fluid.

(3) If $\gamma_1\neq 0$ and $\gamma_2=0$, then the model is reduced to convected Maxwell model. This model also used for viscoelastic flow calculation because of its simplicity.

(4) For $\gamma_1=0$ and $\gamma_2\neq 0$, the model simplified to second-order fluid.

Let $\boldsymbol{x}=(x_1,x_2,x_3)$ and set the velocity and an orientation stress tensor:

$$\boldsymbol{v}(\boldsymbol{x},t)=[\boldsymbol{v}_1,\boldsymbol{v}_2,\boldsymbol{v}_3]^{\mathrm{T}},\quad \boldsymbol{M}(\boldsymbol{x},t)=\begin{bmatrix} M_{11} & M_{12} & M_{13}\\ M_{21} & M_{22} & M_{23}\\ M_{31} & M_{32} & M_{33}\end{bmatrix}, \tag{17}$$

where $M(\boldsymbol{x},t)$ is symmetric. The viscosity of the blood is $\eta(h,d)$ which is a function of the vessel diameter and the hematocrit. The second equation of the system (13) is a tensor equation equivalent to nine scalar equations corresponding to the components σ_{ij} given by

$$\sigma_{ij}=-pI_{ij}+\eta(h,d)\left(\frac{\partial\boldsymbol{v}_i}{\partial x_j}+\frac{\partial\boldsymbol{v}_j}{\partial x_i}\right)+gM_{ij},\quad i,j=1,2,3. \tag{18}$$

In order to calculate the orientation stress tensor, first we consider all components of the orientation stress tensor M and then find the solution to the second equation of the reformulated Oldroyd-B model in eq. (16) with the expression of velocity $\boldsymbol{v}$ and the orientation stress tensor M in eq. (14):

$$\begin{aligned} &\frac{\partial M_{ij}}{\partial t}+\sum_{k=1}^{3}\left[\boldsymbol{v}_k\frac{\partial M_{ij}}{\partial x_k}-M_{ik}\frac{\partial\boldsymbol{v}_j}{\partial x_k}-M_{kj}\frac{\partial\boldsymbol{v}_i}{\partial x_k}\right]\\ &\quad=\frac{1}{\tau}\left(\frac{\alpha(t)\delta_{ij}}{(6\pi a\eta(h,d))^2}-M_{ij}\right),\ i,j=1,2,3. \end{aligned} \tag{19}$$

Here δ_{ij} is the Kronecker delta. All nine components of the orientation stress tensor M can be determined from eq. (17). The momentum equation in eq. (13) becomes

$$\begin{aligned} &\rho\frac{\partial\boldsymbol{v}_i}{\partial t}+\sum_{j=1}^{3}\boldsymbol{v}_j\frac{\partial\boldsymbol{v}_i}{\partial x_j}\\ &\quad=-\frac{\partial p}{\partial x_i}+\eta(h,d)\left[\sum_{j=1}^{3}\left(\frac{\partial^2\boldsymbol{v}_i}{\partial x_j^2}+\frac{\partial^2\boldsymbol{v}_j}{\partial x_i\partial x_j}\right)\right]\\ &\qquad+g\sum_{j=1}^{3}\frac{\partial M_{ij}}{\partial x_j},\qquad i,j=1,2,3. \end{aligned} \tag{20}$$

In order to obtain the components of the orientation stress tensor M, first, we solve eq. (19) and then we substitute those components of M in eq. (20) to obtain the pressure p. We investigate the total tensor σ once we obtain the orientation stress tensor M and the pressure p. In the one dimensional case, the nonlinear system is easily solved but in higher dimensions, we require some accurate and efficient iterative methods to solve the desired system.

3 Numerical simulation

In this section we use an iterative method to find the numerical solution. Several mixed and semi-implicit methods have been proposed to get more efficient solvers while preserving a high degree of stability and the possibility to use large time steps. The blood flow in the vessel is symmetric at low values of the Reynolds number. As the Reynolds number increases, the blood flow changes from a steady state to an unsteady state. We can apply either a steady state or an unsteady (time dependent) solver to capture these effects as appropriate. Here, we consider that the unsteady shear flow depends only on x_3 and t:

$$\boldsymbol{v}(\boldsymbol{x}, t) = (0, 0, \mu \sin(\omega t) x_3),$$

where μ is the amplitude of the pulsatile component and ω is the frequency. The initial and boundary conditions of velocity on the vessel wall are taken as:

$$\begin{aligned} &\boldsymbol{v}(\boldsymbol{x}, t) = 0 \quad \text{at} \ \ t = 0 = x_3, \\ &\frac{\partial \boldsymbol{v}(\boldsymbol{x}, t)}{\partial x_3} = 0 \quad \text{at} \ \ x_3 = R, \end{aligned} \tag{21}$$

where R is the radius of the vessel. Also we consider some simplifications in the orientation stress tensor components such that $M_{11} = M_{12} = M_{22} \simeq 0$. Thus, eq. (19) becomes

$$\begin{aligned} &\frac{\partial M_{13}}{\partial t} + \mu \sin(\omega t) x_3 \frac{\partial M_{13}}{\partial x_3} + \mu \sin(\omega t) M_{13} = -\frac{1}{\tau} M_{13}, \\ &\frac{\partial M_{23}}{\partial t} + \mu \sin(\omega t) x_3 \frac{\partial M_{23}}{\partial x_3} + \mu \sin(\omega t) M_{23} = -\frac{1}{\tau} M_{23}, \\ &\frac{\partial M_{33}}{\partial t} + \mu \sin(\omega t) x_3 \frac{\partial M_{33}}{\partial x_3} + 2\mu \sin(\omega t) M_{33} \\ &\quad = \frac{1}{\tau}\left(\frac{\alpha(t)}{(6\pi a \eta(h, d))^2} - M_{33}\right), \end{aligned} \tag{22}$$

where $\eta(h, d)$ is the viscosity of the vessel. In order to find the numerical solution to eq. (20), first we solve eq. (22) to obtain the orientation stress tensor component M_{33}. The momentum equation (20) becomes

$$\rho\mu\omega \cos(\omega t) x_3 + (\mu \sin(\omega t))^2 x_3 = -\frac{\partial p}{\partial x_3} + g \frac{\partial M_{33}}{\partial x_3}. \tag{23}$$

For the purpose of numerical computations of the desired quantities, the parameter $\mu = 0.5$ kg cm^{-2} s^{-2}, $\rho = 1.024 \times 10^3$ kg cm^{-3}, $\eta(0.45, 1) = 5.0380P$, $g = 1.13616$ dyn-cm and $\omega = 7.2$ Hz have been used. A complete schematic scenario of the blood flow in a vessel is represented in the given figures. The numerical result in Figure 1 represents the orientation stress tensor component M_{13}. The numerical results of the orientation stress tensor component M_{23} are similar to the orientation stress tensor component M_{13}. Also we know that the matrices are symmetric, that is, M_{13}=M_{31} and M_{23}=M_{32}. Figure 2 represents the orientation stress tensor component M_{33} with the configuration of Brownian force. The surface of the orientation stress tensor M_{13} is not similar to the orientation stress tensor M_{33}, which shows that all components of stress are not equal inside the vessel. If there is no stress on the vessel wall then the flow is incompressible, which represents that the diameter of the vessel is constant.

Figure 3 shows the total stress tensor σ_{33} with the orientation stress tensor M_{33}, which is the numerical result of the first order nonlinear partial differential equations obtained from eqs. (22) and (23). In the absence of the orientation stress tensor, first we calculate the pressure of the vessel from the momentum equation. Then, we substitute the value of the pressure in eq. (23) to obtain the total stress tensor represented in Figure 4. The solution profiles of the total tensor with and without the orientation stress tensor at $x_3 = 0.5$ and

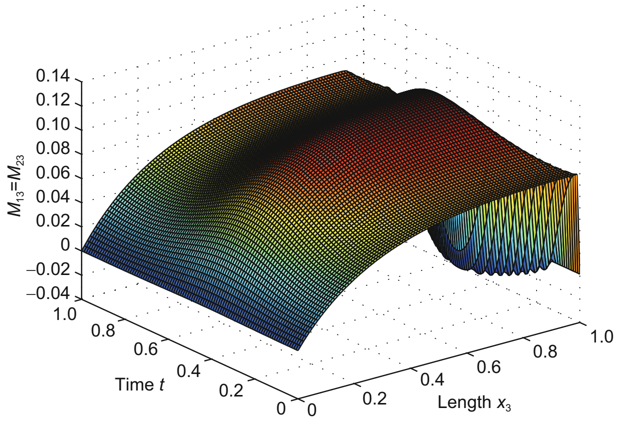

Figure 1 (Color online) The graph represents the orientation stress tensor component M_{13}.

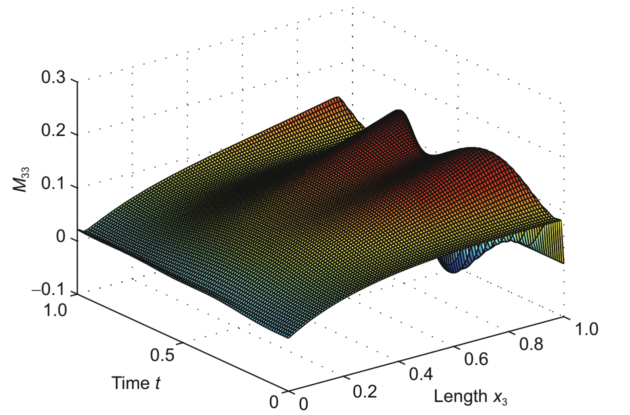

Figure 2 (Color online) The graph represents the orientation stress tensor component M_{33}.

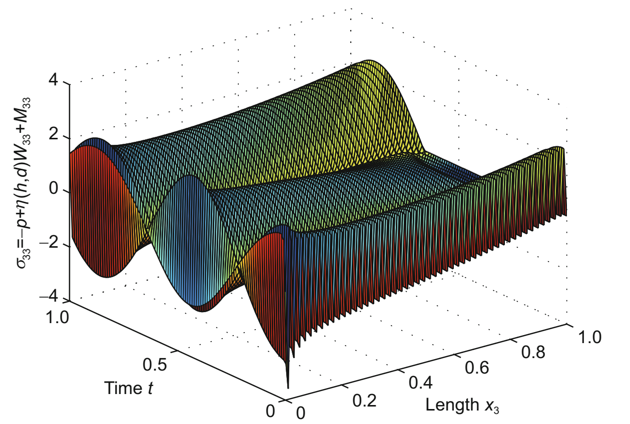

Figure 3 (Color online) The model shows the total stress tensor component with the orientation stress tensor component M_{33} of the vessel.

t = 0.2 are represented in Figures 5 and 6, respectively. The numerical results show that the effect of the orientation stress tensor in a blood vessel is considerable, although the Brownian force is sufficiently small. The total stress tensor σ can be obtained from the pressure, velocity, and the Brownian force. By comparison, with the matrix components in the third equation of the system (13) we determine the components of the total stress tensor

$$\sigma_{13} = \sigma_{23} = \sigma_{31} = \sigma_{32} = gM_{13}(t, x_3),$$
$$\sigma_{13} = 0 = \sigma_{23},$$
$$\sigma_{33} = 2\eta(h, d)\mu \sin(\omega t) + gM_{33}(t, x_3) - p(t, x_3).$$

Note that for numerical simulation, we consider only velocity in the x_3-axis which shows that the magnitudes of all of the components of stress are not similar. Hence, examining all of the results from the present figures, we can estimate the effects of the total stress tensor, the orientation stress tensor, pressure, viscosity, and the nonhomogeneity of blood on the flow phenomena quantitatively in order to validate applicability of the present mathematical model. Furthermore, for a rigid wall problem, only the velocity field requires the initial conditions. However, for the deformable wall problem, both the initial values for the displacement and velocity field are considered. We plan to orient extensions to the current study toward seeking solutions up to critical levels of the total stress tensor, and considering the temporal adjustment of the parameters in the model with the Brownian force.

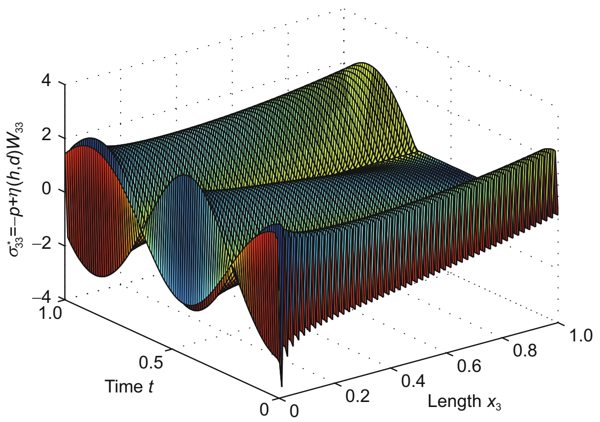

Figure 4 (Color online) The model shows the total stress tensor component σ_{33} without the orientation stress tensor component of the vessel.

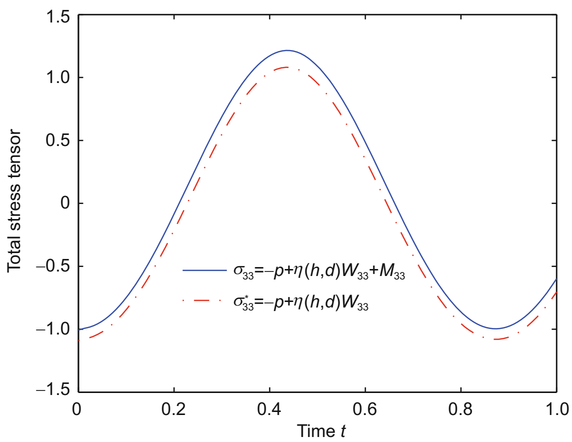

Figure 5 (Color online) Relationship between the total stress tensor component σ_{33} with and without the orientation stress tensor component M_{33} at x_3=0.5.

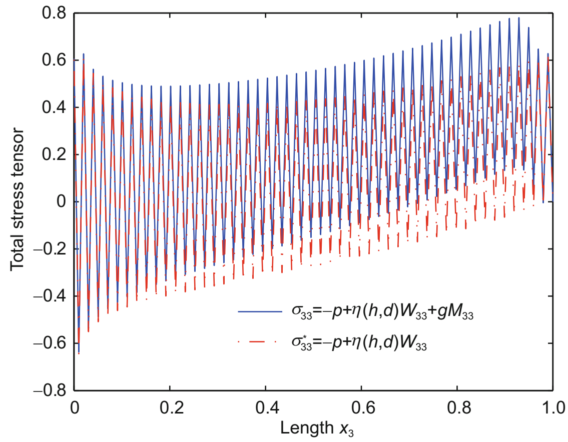

Figure 6 (Color online) Relationship between the total stress tensor component σ_{33} with and without the orientation stress tensor component M_{33} at t = 0.2.

4 Conclusion

In this paper first we considered the Brownian force to derive the orientation stress tensor. The model we developed in this work is a full Oldroyd-B fluid describing the motion of a non-Newtonian incompressible fluid moving into a blood vessel. Then, we showed by numerical simulations that the effect of the orientation stress tensor in the blood vessel is considerable, although the Brownian force is sufficiently small. We also presented the results in the form of a total stress tensor that increases with velocity profiles. Since, the blood flow through a narrow vessel is often pulsatile, the extension of this work to pulsatile flow could be more useful. The applications of such models are important to the real world, because stresses are quite difficult to measure experimentally. Therefore, it is useful to examine them by mathematical models to obtain further insight into aspects of hemodynamics.

This work was supported by the Basic Science Research Program through the National Research Foundation (NRF) of Korea funded by the Ministry of Education, Science and Technology (MEST) (Grant No. 2009-0074305).

1 Humphrey J D. Cardiovascular Solid Mechanics Cell, Tissues and Organs. Heidelberg: Springer-Verlag, 2002
2 Oldroyd J G. On the formulation of rheological equation of state. In: Proceedings of R. S. London A. 1950, 200: 523–541

3 Oldroyd J G. Non-Newtonian effects in steady motion of some idealized elastico-viscous liquids. In: Proceedings of R. S. London A. 1958, 245: 278–297

4 Fung Y C. Biomechanics: Circulation. 2nd ed. New York: Springer-Verlag, 1996

5 Humphrey J D. Mechanics of the arterial wall: Review and directions. Crit Rev Bimed Eng, 1995, 23: 1–162

6 Jung H, Choi J W, Park C G. Asymmetric flows of non-Newtonian fluids in symmetric stenosed artery. Korea-Australia Rheol J, 2004, 16: 101–108

7 Lee S W, Sohn S M, Ryu S H, et al. Experimental studies on the axisymmetric sphere-wall interaction in Newtonian and non-Newtonian fluids. Korea-Australia Rheol J, 2001, 13: 141–148

8 Mekheimer K S. Effect of the induced magnetic field on peristaltic flow of a couple stress fluid. Phys Lett A, 2008, 372: 4271–4278

9 Pontrelli G. Blood flow through a circular pipe with an impulsive pressure gradient. Math Mod Meth Appl Sci, 2000, 10: 187–202

10 Pontrelli G. Blood flow through an axisymmetric stenosis. Proc Inst Mech Eng Part H-J Eng Medicine, 2001, 215: 1–10

11 Quarteroni A. What mathematics can do for simulation of blood circulation. MOX Report, Jan 16, 2006

12 Bellert S L. Computational Fluid Dynamics of the Human Carotid Bifuraction. B. E. Thesis. Brisbane: University of Queensland, 2001

13 Pries A R, Neuhaus D, Gaehtgens F P. Blood viscosity in tube flow: Dependence on diameter and hematocrit. Am J Physiol, 1992, 263: H1770–H1778

14 Fung Y C. Biomechanics: Mechanical Properties of Living Tissues. New York: Springer-Verlag, 1993

15 Song Y S, Youn J R. Modeling of rheological behavior of nanocomposites by Brownian dynamics simulation. Korea-Australia Rheol J, 2004,16: 201–212

16 Wilson H J. Polymeric Fluid Lecture. GM05 part 1, Jan 9, 2006

17 Underhilla P T, Doyle P S. Accuracy of bead-spring chains in strong flows. J Non-Newtonian Fluid Mech, 2007, 145(2-3): 109–123

18 Everitt S L, Harlen O G, Wilson H J, et al. Bubble dynamics in viscoelastic fluids with application to reacting and non-reacting polymer foams. J Non-Newtonian Fluid Mech, 2003, 114: 83–107

19 Yeleswarapu K K, Kameneva M V, Rajagopal K R, et al. The flow of linebreak blood in tubes: Theory and experiment. Mec R Comm, 1998, 25: 257–262

20 Chakravarty S, Sannigrahi A K. A nonlinear mathematical model of blood flow in a costricted artery experiencing body acceleration. Math Com Mod, 1999, 29: 9–25